AN IMAGE MATCHING SCHEME USING A HYBRID FEATURE- AND AREA BASED APPROACH

Nick van der Merwe and Heinz Rüther

Department of Surveying and Geodetic Engineering
University of Cape Town
South Africa
ruther@engfac.uct.ac.za
nvdmerwe@csir.co.za

Commision V, Working Group 3

ABSTRACT

This paper introduces a hybrid image matching scheme that combines aspects of Feature Based Matching (FBM) with Area Based Matching (ABM). Line features are extracted from the images using edge detection followed by line following. These line features are classified using a descriptor function, the $d\phi(s)$ plot. The results of the feature classification determine which features are considered to be suitable matching candidates. Matching feature candidates are matched in a novel, two-step matching process. In the first step the matching probabilities are found by calculating the normalized cross-correlations between the signature functions of the reference and candidate features. In the second step these matching probabilities are used in conjunction with the feature topology to verify feature matches. The results of the feature matching process gives a sparse point field of matching feature centre-of-mass points, which are used to calculate the initial relative orientation. This orientation information is used to find more matching features and to subsequently update the relative orientation. The final, high accuracy relative orientation is calculated from sub-pixel matched corners of matching feature pairs. In the final step the matched features, matching corner points and the relative orientation information is combined to match points on the feature boundaries.

1 INTRODUCTION

In the field of image matching, research has tended to treat area-based and feature-based matching as alternate techniques. In this paper, a hybrid image matching technique is presented that incorporates aspects of both feature- and area based matching without any prior knowledge of the image orientation parameters. A coarse-to-fine approach is used throughout the matching and subsequent relative orientation calculation. Feature matching is used to drastically reduce the search-space for corresponding points, and the results of the feature matching stage are used to calculate an initial estimate of the relative orientation. Once the initial relative orientation has been determined the relative orientation is refined using a combination of feature- and area based matching and the epipolar conditions. The final point matches on the matched feature outlines are also obtained in this way.

One of the major strengths of the feature matching algorithm presented here is its use of not only the local structure of a feature, but also the spatial relations between a feature and its neighbours. Schenk et al[17] presented a method for matching line-features using $\phi(s)$ plots. Horaud and Skordas were one of the first groups to recognize the importance of not only the local structure of a line feature but also the relationship between line features and their surrounding features [13]. Hellwich and Faig improve on the relational matching scheme presented by Horaud and Skordas by extending it to curved lines and avoiding the use of epipolar constraints [11] [12]. One of the first formulations of the image matching solution as a combination between area based matching and feature based matching was by Cochran and Medioni [3], who use image pyramids that are resampled in epipolar geometry to perform a coarse-to-fine match.

This paper will describe the image matching steps of feature extraction, feature classification, feature matching, relative orientation calculation and finally the matching of points on the feature outlines. The main emphasis of this paper will be on the feature matching step, which involves a novel, two-stage matching algorithm that incorporates both the local geometry and topology of line features.

2 FEATURE EXTRACTION

Line features are extracted from the original greyscale images through edge detection with subsequent line following. Once the pixel-level line features have been extracted, the feature boundaries are recalculated to the sub-pixel level.

The edge detector used is the Canny edge detector [2], which calculates the gradient of the input signal with Gaussian smoothing as an integral part of the operator. The level of smoothing is determined by the σ of the Gaussian function.

Edge pixels (edgels) are linked together using an edge-linking algorithm that is similar to chaincodes [6], with enhancements to predict the locus of the next linking pixel and to handle gaps in the edge chain.

The edgels of the pixel-level line features are recalculated to the sub-pixel level using a preservation-of-moments-based edge detector (Tabatabai et al [19]).

The steps of feature extraction and feature classification are described in more detail in a previous paper by the authors [20].

3 FEATURE CLASSIFICATION

Features are classified using a descriptor function, the $d\phi(s)$ function, which is the first-derivative of the $\phi(s)$ function. The $\phi(s)$ function plots the tangential direction of a curve

703

International Archives of Photogrammetry and Remote Sensing. Vol. XXXI, Part B3. Vienna 1996

as a function of the distance travelled around the curve [16]. It indicates abrupt changes of direction as breakpoints in the curve. These breakpoints are indicated as local maxima in the first-derivative of the $\phi(s)$ function, representing the corners of the feature outline.

Using the feature descriptor function, features are classified according to their *size, type* and *number of corners.*

The *size* of a feature is the length of the feature outline in pixels.

The feature *type* broadly classifies a feature into three basic types, namely ARCS, CIRCLES and POLYGONS. An ARC is a linked edge chain that has two nodes at spatially separated endpoints, i.e. an open line feature. A POLYGON is a closed line feature where the start and end nodes are at the same point. A CIRCLE is defined as a polygon that has zero corners and with the ratio between the mean and standard deviation of the $d\phi(s)$ plot below a certain level. Ideally, the $d\phi(s)$ plot for a circle should be a horizontal line, but due to the discrete nature of the input data there is some variation around the mean value, which is quantified by the standard deviation.

The *number of corners* of a feature is calculated from the local maxima of the $d\phi(s)$ plot. Prominent local maxima of the $d\phi(s)$ plot indicate a prominent corner, and statistically-based thresholds are calculated to ensure that only these corners are detected.

The reader is referred to figure 1 for a plot of the LEFT and RIGHT image features after feature extraction and classification. The image features are obtained from a stereo pair of printed circuit board (PCB) images.

The features have been classified and the results of the classification can be found in table 1. For ease of comparison the Feature Classification Table has been arranged so that matching LEFT and RIGHT images features appear next to each other with corresponding numbers for ease of interpretation. Throughout this paper examples using LEFT features labelled L.. and RIGHT features labelled R.. will refer to the features as labelled in figure 1.

Note that only polygons (P) and circles (C) have been used in this example. Arcs were very seldomly repeated in the right image and were thus not used in the feature matching scheme.

4 FEATURE MATCHING

The results of the feature classification stage are used to find suitable matching feature candidates during a candidate selection phase. These matching candidates are then matched using a novel two-stage matching process. In the first step an ordered "feature correspondence table" is generated. This table orders the matching probabilities between reference features and the matching candidates by calculating the normalized crosscorrelations between the feature signature functions. In this case the $d\phi(s)$ function was used as feature signature function, but any suitable signature function could be applied. During the second step the resultant matching probabilities are used in conjunction with the feature topology to verify feature matches. The feature topology is utilized by forming triangles between the centre-of-mass points of the reference feature and the centre-of-mass points of its nearest neighbours in the left (L) image. The matching probabilities obtained from the first matching step indicate the features

L	Type	Size	Corn	R	Type	Size	Corn
L6	P	50	3	R6	P	48	4
L8	P	237	4	R8	P	221	4
L10	P	104	4	R10	P	102	4
L14	P	69	3	R14	P	69	4
L19	P	283	5	R19	P	268	6
L21	P	71	3	R21	P	73	3
L25	P	94	4	R25	P	87	4
L29	P	160	4	R29	P	157	4
L32	P	74	3	R32	P	71	3
L33	P	288	4	R33	P	273	4
L40	P	113	4	R40	P	115	4
L46	P	311	4	R46	P	303	4
L57	P	116	4	R57	P	105	4
L58	C	60	0	R58	C	61	0
L62	C	61	0	R62	C	56	0
L64	C	53	0	R64	C	51	0
L65	C	56	0	R65	P	67	3
L67	P	56	4	R67	P	50	2

Table 1: Feature Classification Table for matching LEFT and RIGHT image features

of which the centroids could form the matching triangle in the candidate image. The existence of a matching triangle verifies the feature match.

In the following the details of the candidate selection and subsequent two-stage feature matching is described in more detail.

4.1 Candidate Selection Phase

To distinguish the feature candidates that are suitable for matching to a specific reference feature the feature attributes of *size, type* and *number of corners* are compared.

A matching candidate has to fulfil the following criteria:

- The feature sizes should differ by no more than ten percent
- The number of corners should differ by no more than one
- The feature types should be the same

Candidates that do not fulfil all of these criteria are immediately eliminated from the matching scheme. Successful candidates now go through the following, two-step procedure:

4.2 Matching $d\phi(s)$ Signatures Through Correlation

In the field of signal processing a measure that gives an indication of the similarity between two random signals is the *Correlation* function [14] [18]. The $d\phi(s)$ plots from different images should be similar for the same feature, and the correlation function can be used to quantify this similarity. The $d\phi(s)$ plot is a one-dimensional function representing the two-dimensional shape of the feature, and the "time" variable used in this case is "s", the distance travelled along the feature boundary.

The time-domain correlation function for two discrete functions $g[n]$ and $h[n]$ of length N is defined as:

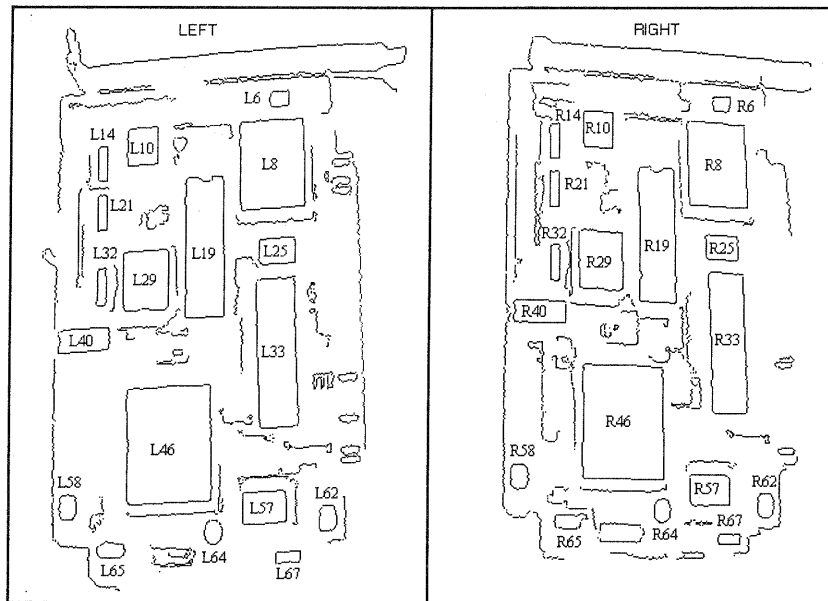$$\Phi_{gh}[n] = \sum_{m=0}^{N-1} g[n+m]h[m] \tag{1}$$

704

Figure 1: LEFT and RIGHT image features after extraction and classification

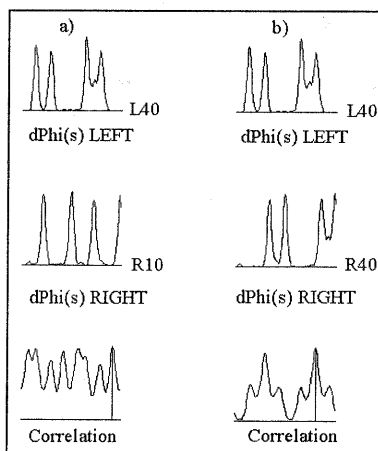where n is the lag in samples between the two data sets.

Figure 2: Time-domain correlation functions between a) L40 and R10 and b) L40 and R40

Figure 2 shows the $d\phi(s)$ plots for feature L40 in the left image compared with features R10 (2 a)) and R40 (2 b)) together with their respective correlation functions derived through time domain correlation. The L40/R10 correlation function has a number of peaks with a maximum correlation value of 54.4 %. The L40/R40 correlation function displays two local maxima peaks, with a maximum correlation value of 95.3 %. are registered due to the symmetry of a rectangular feature about its centroid. Note that the plots in 2 are not according to the same scale.

The $d\phi(s)$ plot is invariant under rotation and translation, but the "s" or "time" axis is stretched and compressed due to the scale. To take the scale difference between the left and right images into account the $d\phi(s)$ plots are resampled to the same length. Only one of the two functions being correlated needs to be resampled to the same length as the other to correct for the scale difference. Resampling can be done through bilinear interpolation or some other resampling method.

For signals of length N, the time-complexity of time-domain correlation is calculated to be N^2, which could be computationally expensive for large features. A method of correlation that is computationally less expensive is using Fast Fourier Transforms (FFTs).

In the frequency-domain, the Fourier Transform $\Phi_{gh}(\Omega)$ of the correlation function can be related to the Fourier Transforms $G(\Omega)$ and $H(\Omega)$ of the discrete signals $g[n]$ and $h[n]$ as:

$$\Phi_{gh}(\Omega) = G(\Omega)H^*(\Omega) \qquad (2)$$

where $H^*(\Omega)$ is the complex conjugate of $H(\Omega)$.

For real valued functions such as the "$d\phi(s)$" plots the imaginary part of the signal is zero and the complex conjugate is simply $H(-\Omega)$.

The discrete-time correlation function $\Phi_{gh}[n]$ can now be reconstructed by calculating the Inverse Fourier Transform of $\Phi_{gh}(\Omega)$. The resultant maximum correlation values calculated from this reconstructed correlation function are 54.4% and 95.3% respectively, exactly the same as for time-domain correlation.

The FFT algorithm requires the input data set to be of an integral power of two in length. The next integral power of two above the feature size in pixels is calculated for each of the left feature and the right candidate, and the $d\phi(s)$ functions are resampled to this value. This resampling again takes into account the scale difference between the left and right images.

The output of the cross-correlation between signals $g[n]$ and $h[n]$ cannot be compared as is, as it is dependent on the width N of the sequence and the scale. To obtain a quantity that can be used for comparison we have to normalize the cross-correlation output. This normalized quantity can directly be used for matching purposes and is called the cor-

705

relation coefficient.

The correlation coefficient ρ is normalized by taking into account the autocorrelations of the signals $g[n]$ and $h[n]$. The correlation between a function and itself is called the *autocorrelation*, which is used to calculate the amount of power contained in the signal.

$$\rho = \frac{(\Phi_{gh})_{max}}{\sqrt{\Phi_{gg}\Phi_{hh}}} \qquad (3)$$

where Φ_{gh} is the crosscorrelation between $g[n]$ and $h[n]$ and Φ_{gg} and Φ_{hh} are the autocorrelations for $g[n]$ and $h[n]$ respectively.

From the correlation coefficients between the LEFT features and all potential matching RIGHT features a Feature Correlation Table is obtained which orders the possible matches according to the correlation coefficients. The correlation coefficients between left and right features are expressed as a percentage. Only the two most probable candidates are shown in the Feature Correlation Table (2) for the printed circuit board (PCB) example .

Left	Right1	Correlation	Right2	Correlation
L6	R6	94.12	R67	88.41
L8	R8	95.23	R33	59.61
L10	R10	96.11	R57	93.72
L14	R14	99.41	R32	98.43
L19	R19	92.59	R33	83.38
L21	R32	98.98	R14	96.79
L25	R57	95.55	R25	93.86
L29	R29	90.01	-	-
L32	R32	86.72	R65	85.17
L33	R33	87.05	R46	58.53
L40	R40	95.35	R57	64.18
L46	R46	97.21	R33	55.25
L57	R57	96.18	R10	89.88
L58	R62	94.55	R58	93.25
L62	R62	95.63	R58	94.51
L64	R64	98.37	R62	93.83
L65	R62	91.14	R64	88.96
L67	-	-	-	-

Table 2: Ordered Feature Correlation Table for Feature Matching Candidates

This table indicates that for example the feature L6 has most likely matching candidate R6 with a "probability" of 94.12%, and second most likely matching candidate R67 with a "probability" of 88.41%. Throughout this paper the examples used in the analysis of feature correlation will refer to table 2.

4.3 Match Verification Through Feature Topology

In the second step of the feature matching stage the possible feature matches stored in the Feature Correlation Table are either verified or discarded by examining the feature topology. Where the $d\phi(s)$ plot only takes into account the local shape of the feature, the feature topology also considers the spatial relationship between a feature and its neighbours.

The method of *similar triangles* as described by Cox *et al* in [5] for point pattern recognition was used to find the spatial relationship between adjacent features.

Feature triangles are formed between the reference feature and two adjacent features. The two nearest features to the reference feature are found and a triangle is formed with its vertices at the centre-of-mass points (centroids) of each feature. Refer to figure 3 for an example of a feature triangle between the reference feature $f1$ and the two nearest features $f2$ and $f3$. The corresponding feature triangle T_2 between the corresponding features f_1', f_2' and f_3' in the RIGHT image is also shown.
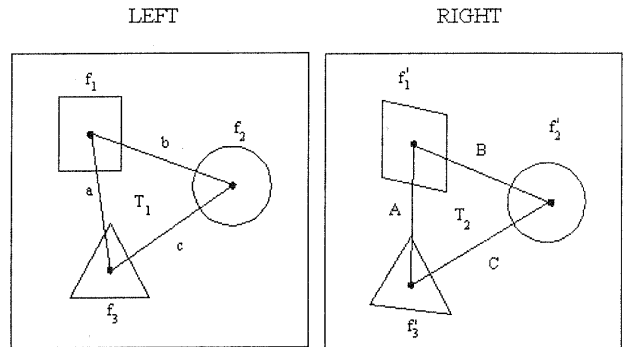

Figure 3: Triangle between feature f1 , f2 and f3

If the corresponding triangle T_2 can be found amongst the possible triangle combinations in the RIGHT image then the match is verified. The possible triangle combinations are determined by the ordered feature correlation table (2). The feature triangle takes into account not only the topology between the reference feature f_1 and its surrounding features, but also the topology between features f_2 and f_3. Even though a matching triangle implies that the two neighbouring features also match, only the initial candidate feature match is verified.

Triangle T_1 matches triangle T_2 if

$$\frac{a}{b} = \frac{A}{B} \quad \text{and} \quad \frac{b}{c} = \frac{B}{C} \qquad (4)$$

within a preset threshold, where a, b, c and A, B, C are corresponding triangle sides.

The same is true for corresponding angles. If two of the three angles of the triangle are the same then a matching triangle is found. In this matching scheme only the distance ratios are used.

Feature matching candidates are confirmed or discarded by comparing triangles formed between the most likely matching candidates. To find the triangle in the RIGHT image that matches the reference triangle in the LEFT image the possible triangle combinations are deduced from the Feature Correlation Table (Table 2). For a successful match to a reference feature at least one possible matching candidate should be listed in the Feature Correlation Table. In this example only features that are classified as POLYGONS or CIRCLES are used to form feature triangles. Due to spatial and radiometric differences between the left and right images many features labelled as ARCs do not have a matching pair, which would lessen the chance of the matching triangle being formed.

In general not all the features will have the same number of matching candidates. If a threshold is set to only select

706

International Archives of Photogrammetry and Remote Sensing. Vol. XXXI, Part B3. Vienna 1996

candidates with a high correlation value, then only the valid candidates for each feature in the reference triangle need to be checked. If the features f_1, f_2 and f_3 of figure 3 have I, J and K valid matching candidates respectively then the total number of possible triangle combinations will be $I * J * K$. Note that for the example shown above only the two most likely candidates are indicated thus $I = J = K = 2$, giving a total of eight possible triangle combinations.

L25	L8	L19
R57	R8	R19
R57	R8	R33
R57	R33	R19
R57	R33	R33
R25	*R8*	*R19*
R25	R8	R33
R25	R33	R19
R25	R33	R33

Table 3: Possible Matching Triangle Combinations for the Triangle L25-L8-L19

Table 3 shows the possible triangle combinations that can be formed to verify the match between features L25 and R25. The reference triangle has been formed between features L25, L8 and L19. From table 2 the possible matching triangle combinations can now be formed, as indicated in table 3. This table is arranged such that the most likely matching triangle is checked first through to the least likely matching triangle last. The correct triangle combination R25-R8-R19 has been highlighted in table 2. Note that illegal triangle combinations can be formed, such as the fourth combination R57-R33-R33, which is automatically discarded by the matching algorithm. In this specific example the first four entries in table 3 have R57 as the most likely matching candidate for L25. As R57 in figure 1 is situated far from the correct match R25, the scale limit between the two triangles will be violated and all four combinations will automatically be discarded. The scale limit has been introduced to further reduce the search space by limiting the size difference between corresponding sides of the reference and candidate triangles to no more than twenty percent.

L25   R25

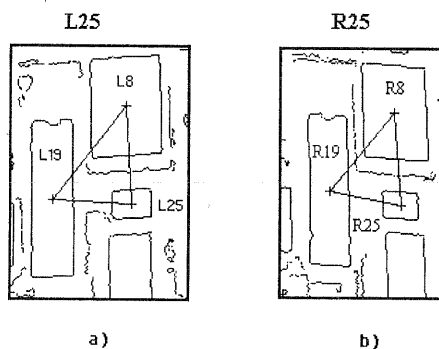

a)   b)

Figure 4: Similar Triangles for L25 a) and R25 b)

The reader is referred to figure 4 for the matching triangles verifying the match between features L25 and R25. The nearest neighbours to L25 in the LEFT image are L8 and L19 respectively, with the feature triangle between the centroids

of these features shown in figure 4 a). The corresponding triangle in the RIGHT image joins the centroids of R25, R8 and R19 shown in figure 4 b). Table 2 indicates that R25 is the second most likely matching candidate for L25, R19 is the most likely matching candidate for L19 and R8 is the most likely matching candidate for L8. The confidence index for the correct match is 94.30 %. Even though R25 was not the most likely matching candidate the correct match was still found.

The sides of the reference triangle have been arranged in ascending order in size such that

$$a \leq b \leq c \qquad (5)$$

as suggested by Cox and de Jager [4].

This has the effect of limiting the ratios used for triangle comparison to the range between zero and one i.e.

$$0 < \frac{a}{b} \leq 1 \quad \text{and} \quad 0 < \frac{b}{c} \leq 1 \qquad (6)$$

A *confidence index* is introduced to quantify the similarity between triangles, and is calculated using the Euclidean distance between the triangle side ratios. The Euclidean distance ε between the triangle side ratios is

$$\varepsilon = \sqrt{(\frac{a}{b} - \frac{A}{B})^2 + (\frac{b}{c} - \frac{B}{C})^2} \qquad (7)$$

which is the error vector between the left and right triangle ratios.

The error vector ε can be normalised by introducing the theoretical minima and maxima of equation (7). The minimum value for equation (7) ($\varepsilon_{min} = 0$) occurs when the matched triangles are identical. A maximum for equation (7) arises for $\frac{a}{b} = \frac{b}{c} = 1$, i.e. an equilateral triangle, and $\frac{A}{B} = \frac{B}{C}$ close to 0, a theoretical case which will not occur in practise. The theoretical maximum is thus $\varepsilon_{max} = \sqrt{2}$.

This normalizing factor of $\sqrt{2}$ is now used to calculate the confidence index CI as

$$CI = 100(1 - \frac{\varepsilon}{\sqrt{2}}) \qquad (8)$$

If the triangle is perfectly matched the Euclidean distance ε is zero and the confidence index is 100 %. As the Euclidean distance increases due to dissimilar triangles the confidence index becomes smaller. It is assumed that corresponding sides have the same relationship as the reference triangle i.e. $A \leq B \leq C$. In practice however this relationship might not hold for an incorrect triangle, which could result in triangle side ratios for the right triangle of greater than one, which could result in negative values for the confidence index. These negative values merely serve as an indication of a very strong mismatch between the reference and candidate triangles.

5 RELATIVE ORIENTATION

The relative orientation is performed using a three step procedure that utilizes a "coarse-to-fine" approach. The first orientation approximation relies on the centroids of the features matched in the previous topology-based matching process.

707

International Archives of Photogrammetry and Remote Sensing. Vol. XXXI, Part B3. Vienna 1996

The epipolar line constraints derived from this first approximate orientation are then employed to find further matches for centroids of features previously not matched successfully. A second, updated relative orientation is executed with these additional points. The newly obtained epipolar constraint is now utilised to match the corner points of all conjugate features by area based matching. A third and final relative orientation incorporating the sub-pixel matched corner points then provides final orientation parameters. The procedure described here is fully automated and does not require any user support.
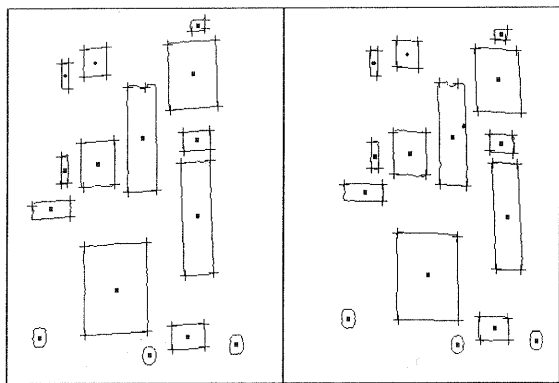

Figure 5: Relative orientation from matching feature centroids and corner points

In the test case of the PCB images thirteen matching feature centroids, indicated as squaresin figure 5, were entered into the first relative orientation. Two further features (the rectangular shapes in the top left corner of the images) were detected in the next stage and a second orientation with these fifteen centroids was successfully executed. For the final relative orientation calculation only the forty five sub-pixel coordinates of the matching corner points, indicated by crosses, were used. During the first two orientations the assumption was made that the centroids of matching features in each image match, which is not entirely accurate. Due to large disparities and the different viewing perspectives for different images, these centroids can only be treated as crude approximations to the matching points, and are thus discarded for the final relative orientation calculation.

The relative orientation and subsequent epipolar line equations are solved for using the coplanarity condition, as described by Haralick and Shapiro [10]. During the corner-matching step, image correlation as described by Rosenfeld and Kak [15] is employed to solve any ambiguities resolving from more than one corner matching candidate appearing on an epipolar line. The sub-pixel corner matches are calculated using Least-Squares Matching (LSM) as described by Gruen *et al* [7] [8] [9].

6 FEATURE-GEOMETRY CONSTRAINED AREA BASED MATCHING

During the final step in the matching procedure intermediate points on the matched feature outlines are matched to sub-pixel level.

The initial estimates to the matching points for points situated on a matched line feature, as opposed to corner points, are obtained by searching for the intersection between the
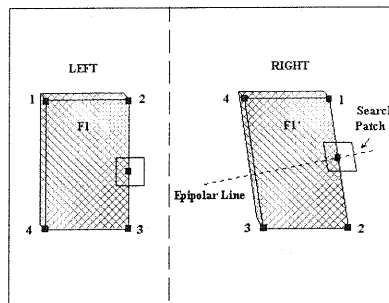
corresponding line feature and the epipolar line.

Figure 6: Initial Maching Point Approximations Using Matching Features and Epipolar Geometry

If in figure 6 the feature matching stage has matched feature F_1 in the left image to feature F_1' in the right image and the subsequent corner matching stage using the epipolar condition and Least Squares Matching has correctly matched the four corner points, then the search space for points on the feature boundary can dramatically be reduced. In this example corners 2 and 3 in the left image match corners 1 and 2 in the right image. The search space for matching points along line 2-3 in the left image is now reduced to line 1-2 in the right image. If any ambiguities occur they are resolved using area correlation, as done with corner matching.

It should be noted that the intersections between feature boundaries and epipolar lines are subject to the well known geometric conditions of the intersection, with best solutions for rectangular intersects and no solutions for paralell lines. Only by using more than two images and therefore more than one epipolar line can this problem be solved.
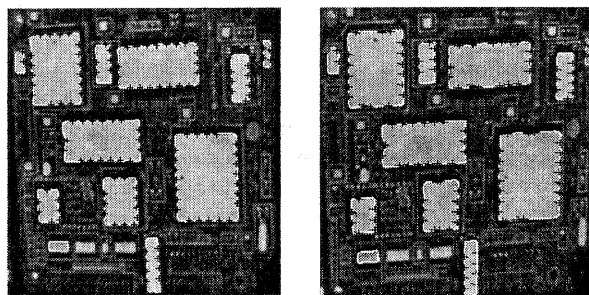

Figure 7: Example of Finding Initial Maching Point Approximations

Figure 7 shows an example of finding the initial matching point approximations for points on matched line features. In this example the initial approximations to every tenth edge element (edgel) of each line segment between feature corners are shown. The edgels are indicated by crosses in the left image and the corresponding point approximations with the relevant epipolar line segments are indicated in the right image. Note that, as expected, the line intersections for line segments parallel to the epipolar lines, which are near-horizontal in this case, are poorly defined as shown in figure 8.

From these initial estimates the high accuracy, sub-pixel matching is performed using LSM or Geometrically Constrained Least Squares Matching (GCLSM), as described by Gruen [7] and Baltsavias [1].
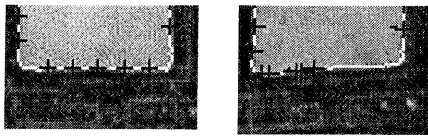
708

International Archives of Photogrammetry and Remote Sensing. Vol. XXXI, Part B3. Vienna 1996

Figure 8: Zoomed Sub-images of Poorly Defined Epipolar Line Intersections

7 CONCLUSION

We have presented an image matching scheme that incorporates both feature- and area based matching techniques. A novel, two-stage feature matching algorithm was presented. The two stages of the matching scheme take into account firstly the local structure of a feature, and secondly the spatial relation between a feature and its neighbours. Combining these two aspects improves on matching schemes that employ only one or the other. We have also shown how feature matching can be used to obtain initial estimates to the relative orientation, effectively enabling us to subsequently refine this relative orientation using a combination of feature- and area based matching and the resultant epipolar geometry. This technique makes it possible to carry out a fully automated relative orientation without any prior knowledge of orientation parameter estimates.

Improvements can be made to this matching scheme, most notably in the handling of ARCs and images with large disparities. Extending this matching scheme to a multi-photo and multi-resolution environment will also help in improving the results obtained.

REFERENCES

[1] E. Baltsavias. *Multiphoto Geometrically Constrained Matching*. PhD thesis, Institute of Geodesy and Photogrammetry, 1991. Mitteilungen nr.49.

[2] J. Canny. "A Computational Approach to Edge Detection". *IEEE Transactions on Pattern Analysis and Machine Intelligence*, PAMI-8(6):679–698, November 1986.

[3] S. Cochran and G. Medioni. "3-D Surface Description from Binocular Stereo". *IEEE Transactions on Pattern Analysis and Machine Intelligence*, 14(10):981–994, 1992.

[4] G. Cox and G. de Jager. "A New Point Pattern Recognition Technique". Technical report, Department of Electrical and Electronic Engineering, UCT, 1994.

[5] G. Cox, G. de Jager, and B. Warner. "A New Method of Rotation, Scale and Translation Invariant Point Pattern Matching Applied to the Target Acquisition and Guiding of an Automatic Telescope". *2nd South African Workshop on Pattern Recognition*, November 1991.

[6] H. Freeman and L. Davis. "A Corner-Finding Algorithm for Chain-Coded Curves". *IEEE Transactions on Computers*, pages 297–303, March 1977.

[7] A. Gruen. "Adaptive Least Squares Correlation - A Powerful Image Matching Technique". *Presented Paper to the ACSM-ASP Convention Washington D.C.*, 42:97–112, March 1985.

[8] A. Gruen and E. Baltsavias. "High-Precision Image Matching for Digital Terrain Model Generation". *Photogrammetria*, 42:97–112, 1987.

[9] A. Gruen and D. Stallmann. "High Accuracy Dimensional Measurement Using Non-Targeted Object Features". *International Archives of Photogrammetry and Remote Sensing*, 29(B5):694–700, 1992.

[10] R. Haralick and L. Shapiro. *Computer and Robot Vision*, volume 1-2. Addison Wesley, 1992.

[11] O. Hellwich and W. Faig. "Graph-Based Matching of Stereo Image Features". *International Archives of Photogrammetry and Remote Sensing*, 29(B3):307–317, 1992.

[12] O. Hellwich and W. Faig. "Graph-Based Feature Matching Using Descriptive and Relational Parameters". *Photogrammetric Engineering and Remote Sensing*, 60(4):443–450, April 1994.

[13] R. Horaud and T. Skordas. "Stereo Correspondence Through Feature Grouping and Maximal Cliques". *IEEE Transactions on Pattern Analysis and Machine Intelligence*, 11(11):1168–1180, November 1989.

[14] A. Oppenheim and R. Schafer. *Discrete - Time Signal Processing*. Prentice-Hall, 1989.

[15] A. Rosenfeld and A. Kak. *Digital Picture Processing*, volume 1-2 of *Computer Science and Applied Mathematics*. Academic Press, Orlando, second edition, 1982.

[16] T. Schenk. "Algorithms and Software Concepts for Digital Photogrammetric Workstations". In D. of Geodetic Science and Surveying, editors, *Technical Notes in Photogrammetry*, July 1992.

[17] T. Schenk, J. Li, and C. Toth. "Towards an Autonomous System for Orienting Digital Stereopairs". *Photogrammetric Engineering and Remote Sensing*, 57(8):1057–1064, August 1991.

[18] F. Stremler. *Introduction to Communication Systems*. Addison-Wesley, second edition, 1982.

[19] A. Tabatabai and O. Mitchell. "Edge Location to Subpixel Values in Digital Imagery". *IEEE Transactions on Pattern Analysis and Machine Intelligence*, PAMI-6(2):188–201, March 1984.

[20] N. van der Merwe and H. Rüther. "Image Matching Through a Combination of Feature- and Area Based Matching". *International Archives of Photogrammetry and Remote Sensing*, 30(5):407–413, March 1994.

709

International Archives of Photogrammetry and Remote Sensing. Vol. XXXI, Part B3. Vienna 1996